analytical chemistry

pubs.acs.org/ac Article

Coupling Anion Exchange Chromatography with Native Mass Spectrometry for Charge Heterogeneity Characterization of Monoclonal Antibodies

Anita P. Liu, Yuetian Yan, Shunhai Wang,* and Ning Li

Cite This: *Anal. Chem.* 2022, 94, 6355−6362 Read Online

ACCESS | Metrics & More | Article Recommendations | Supporting Information

ABSTRACT: Despite the recent success of coupling anion exchange chromatography with native mass spectrometry (AEX-MS) to study anionic proteins, the utility of AEX-MS methods in therapeutic monoclonal antibody (mAb) characterization has been limited. In this work, we developed and optimized a salt gradient-based AEX-MS method and explored its utility in charge variant analysis of therapeutic mAbs. We demonstrated that, although the developed AEX-MS method is less useful for IgG1 molecules that have higher isoelectric points (p*I*s), it is an attractive alternative for charge variant analysis of IgG4 molecules. By elevating the column temperature and lowering the mAb p*I* through PNGase F-mediated deglycosylation, the chromatographical resolution from AEX separation can be significantly improved. We also demonstrated that, after PNGase F and IdeS digestion, the AEX-MS method exhibited excellent resolving power for multiple attributes in the IgG4 Fc region, including unprocessed C-terminal Lys, *N*-glycosylation occupancy, and several conserved Fc deamidations, making it ideally suited for multiple attribute monitoring (MAM). Through fractionation and peptide mapping analysis, we also demonstrated that the developed AEX-MS method can provide site-specific and isoform-resolved separation of Fc deamidation products, allowing rapid and artifact-free quantitation of these modifications without performing bottom-up analysis.

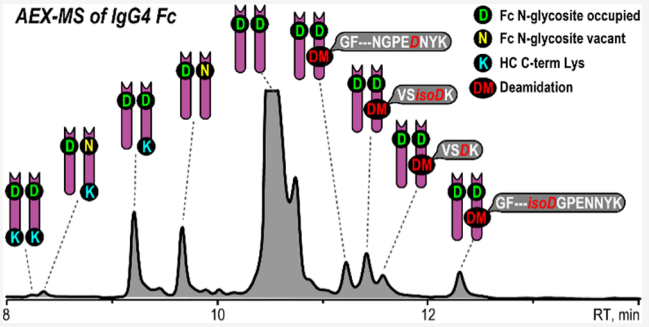

Charge heterogeneity, commonly arising from numerous post-translational modifications, is considered a critical quality attribute in therapeutic monoclonal antibodies (mAbs), and thus, needs to be thoroughly characterized and monitored throughout the drug development stages.[1−3] Ion exchange chromatography (IEX) and capillary electrophoresis (CE) are the two main groups of techniques used to discern the overall charge heterogeneity of mAbs and are routinely employed in QC release to ensure product and process consistency.[4−6] Understanding the biochemical root cause of mAb charge heterogeneity is not only utterly important for out-of-trend (OOT) or out-of-specification (OOS) investigations but it also provides frameworks for risk assessment and opportunities for process improvement. Mass spectrometry (MS)-based tools have played a critical role in this task. Traditionally, offline fractionation by IEX or off-gel isoelectric focusing (IEF) followed by MS-based analyses is a highly effective approach to elucidate the mAb charge heterogeneity, although the process is low throughput and susceptible to artifact formation.[7,8] Recent advances in both instrumentation and methodology have led to successful online coupling of multiple charge-based separation techniques with direct MS detection.[9,10] For example, both capillary zone electrophoresis (CZE)[11] and capillary isoelectric focusing (cIEF)[12,13] have been directly interfaced with MS and applied in mAb charge heterogeneity characterization at both intact and subunit levels. In addition, cation exchange chromatography coupled with native MS (CEX-MS) methods have also gained popularity in recent years. Using ammonium-based volatile salts as mobile phases, the reported CEX-MS methods utilized either pH,[14,15] salt,[16,17] or salt-mediated pH[18,19] gradients for mAb charge variant separation prior to native MS detection. Because of the different separation mechanisms, these three methods (i.e., CZE-MS, cIEF-MS, and CEX-MS) can offer orthogonal selectivity and provide complementary information on mAb charge heterogeneity.

Unlike CEX, anion exchange chromatography (AEX) has not been commonly applied for mAb charge heterogeneity analyses.[20] This is largely due to the fact that the majority of the marketed mAb molecules tend to be relatively basic,[21] making them less suitable to be analyzed by AEX. As a result,

Received: February 11, 2022
Accepted: April 5, 2022
Published: April 14, 2022

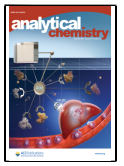

https://doi.org/10.1021/acs.analchem.2c00707
Anal. Chem. 2022, 94, 6355−6362

recently reported applications of native AEX-MS methods have been limited to relatively anionic proteins, such as human serum albumin,[22] ovalbumin,[23] and recombinant erythropoietin.[24] However, it is important to point out that the majority of the marketed therapeutic mAbs belong to IgG1 subclass, which tend to have high p*I*s (>7.5). In contrast, IgG4 molecules, which are playing an increasingly important role as therapeutic candidates, tend to have lower p*I*s,[21] which makes them potentially suitable to be analyzed by AEX-MS methods.

In this study, we developed and optimized a salt gradient-based AEX-MS method and explored its utility in charge heterogeneity characterization of therapeutic mAbs. During the method development, we evaluated different elution modes, column operating temperatures, and sample treatments to improve chromatographical resolution. Several mAb molecules with a wide range of p*I*s, from both IgG1 and IgG4 subclasses, were tested to evaluate the method suitability. We also discovered that after PNGase F and IdeS digestion, the developed native AEX-MS method exhibited excellent resolving power for multiple attributes in the IgG4 Fc region. In particular, this method can resolve site-specific Fc deamidation variants, as well as deamidated isoforms (Asp vs isoAsp), which were further confirmed by peptide mapping analysis of the AEX fractionations.

EXPERIMENTAL SECTION

Materials. IgG1- and IgG4-based mAbs were generated at Regeneron Pharmaceuticals Inc. (Tarrytown, NY). NIST Monoclonal Antibody Reference Material 8671 (NISTmAb, humanized IgG1K monoclonal antibody) was purchased from National Institute of Standards and Technology (Gaithersburg, MD). Ammonium acetate (LC/MS grade), ammonium hydroxide, acetic acid, urea, and iodoacetamide (IAM) were purchased from Sigma-Aldrich (St. Louis, MO). Peptide *N*-glycosidase F (PNGase F) was purchased from New England Biolabs Inc. (Ipswich, MA). FabRICATOR (IdeS) was purchased from Genovis (Cambridge, MA). Sequence grade modified trypsin was purchased from Promega (Madison, WI). Pierce DTT (dithiothreitol, No-Weigh Format), Invitrogen UltraPure 1 M Tris-HCl buffer (pH 7.5), water with 0.1% formic acid (v/v) (Optima LC/MS grade), and acetonitrile with 0.1% formic acid (v/v) (Optima LC/MS grade) were obtained from Thermo Fisher Scientific (Waltham, MA). 2-Propanol (IPA, HPLC grade) was purchased from Honeywell (Muskegon, MI). Synthetic peptides (VSDK, GFYPSDIAVEWESDGQPENNYK, and GFYPSDIAVEWESNGQPEDNYK) were purchased from Genscript (Piscataway, NJ). Deionized water was provided by a Milli-Q integral water purification system installed with a MilliPak Express 20 filter (MilliporeSigma, Burlington, MA).

Sample Preparation. The mAb samples were diluted to 5 mg/mL with water prior to injection for native AEX-MS analysis. For deglycosylated samples, mAbs were treated with PNGase F at 1 IUB milliunit per 10 μg of protein in 100 mM Tris-HCl (pH 7.5) at 45 °C for 1 h prior to native AEX-MS analysis. For subunit analysis, the deglycosylated mAbs were subjected to site-specific digestion with IdeS (1 IUB milliunit per 1 μg of protein) in 100 mM Tris-HCl (pH 7.5) at 37 °C for 1.5 h, to generate the $F(ab)'_2$ and Fc fragments.

Native AEX-MS Methods. AEX chromatography was performed on an UltiMate 3000 UHPLC System (Thermo Fisher Scientific, Bremen, Germany) equipped with an UltiMate 3000 PCM-3000 pH and conductivity monitor. For native AEX-MS analysis, unless otherwise specified, 10 μg of mAb sample was injected onto a YMC-BioPro QA-F SAX column (4.6 mm × 100 mm, 5 μm; YMC Co., Ltd., Kyoto, Japan) at a flow rate of 0.4 mL/min. The column compartment temperature was set at 45 °C for intact mAb analyses and at 25 °C for subunit analyses. For the salt gradient method, mobile phase A was 10 mM ammonium acetate, pH 6.7, and mobile phase B was 300 mM ammonium acetate, pH 6.8. For the salt-mediated pH gradient method, mobile phase A was 10 mM ammonium acetate, pH adjusted to 9.0 using ammonium hydroxide, and mobile phase B was 50 mM ammonium acetate, pH adjusted to pH 4.0 using acetic acid. Upon sample injection, the AEX gradient was held at 100% mobile phase A for 2 min followed by a linear increase to 100% mobile phase B over 16 min. The gradient was then held at 100% mobile phase B for 4 min before returning to 100% mobile phase A to recondition the column. The CEX-MS conditions used for comparison are described in the Supporting Information.

A Thermo Q Exactive UHMR (Thermo Fisher Scientific, Bremen, Germany) equipped with a Microflow-Nanospray Electrospray Ionization (MnESI) source and a Microfabricated Monolithic Multinozzle (M3) emitter (Newomics, Berkley, CA) was used for native MS analysis. A detailed experimental setup and the MS instrument parameters can be found in a previous publication.[25] Raw data from the AEX-MS analysis were deconvoluted using Intact Mass software from Protein Metrics (Cupertino, CA).

Peptide Mapping Analysis of AEX Fractions. The basic, acidic, and main Fc fractions were isolated by collecting the corresponding fractions from AEX separation of the deglycosylated and IdeS-treated IgG4 mAbs. The collected fractions were then subjected to liquid chromatography with tandem mass spectrometry (LC-MS/MS)-based peptide mapping analysis following tryptic digestion using a protocol described in the Supporting Information.

RESULTS AND DISCUSSION

Development of a Native AEX-MS Method. A previously reported native LC-MS platform was adopted for native AEX-MS method development (Figure S1).[25] Briefly, an analytical scale YMC-BioPro QA-F SAX column, which contains nonporous hydrophilic polymer packed with quaternary ammonium groups for strong anion exchange (SAX), was selected for mAb separation. A stainless steel tee was employed to direct the majority of the LC flow to a UV detector, as well as an in-line pH and conductivity monitor. The remaining LC flow (sub-microliter per minute range) was then subjected to nanoelectrospray ionization (NSI) using a Microfabricated Monolithic Multinozzle (M3) emitter. In addition, using isopropyl alcohol (IPA) as a dopant, modified desolvation gas was also applied to the NSI to improve the spray stability. As this developed platform can tolerate high salt concentrations (up to 600 mM ammonium acetate),[25] it provides great flexibility to test the AEX-MS method under different elution modes using various mobile phases.

Initially, we tested a salt-mediated pH gradient from 10 mM ammonium acetate at pH 9.0 to 50 mM ammonium acetate at pH 4.0. Ammonium acetate-based mobile phases were selected because this volatile salt is less likely to denature proteins comparing to other ammonium-based salts (i.e., ammonium bicarbonate),[26] and therefore is highly preferred in native LC-MS applications. Under this elution mode, the mAb molecules are initially deprotonated and bound to the positively charged

https://doi.org/10.1021/acs.analchem.2c00707
Anal. Chem. 2022, 94, 6355−6362

functional groups of the anion exchange resin. As the pH decreases and the ionic strength increases, the elution occurs due to both the neutralization (or even the protonation) of the mAb surface charge and the increased competition for binding from salt ions. As shown in the pH plot recorded by the in-line pH monitor (Figure S2a, blue trace), a "pH drop" can be clearly observed between pH 8.5 and 5.0. This "buffering gap" is expected because ammonium acetate can only provide buffering ranges around pH 4.75 ± 1 (pK_a of acetic acid) and around pH 9.25 ± 1 (pK_a of ammonium).[27] This feature is undesirable for the analysis of mAb molecules, as the majority of them have p*I*s within this range. Indeed, the poor separation performance of this method was confirmed by testing several mAb molecules (data not shown). Next, we evaluated a pure salt gradient using 10 mM ammonium acetate as mobile phase A and 300 mM ammonium acetate as mobile phase B without adjusting the pH. Under this mode, the elution of mAb molecules is solely driven by the increased competition for binding from salt ions. As shown in the conductivity plot (Figure S2b, blue trace), a linear conductivity gradient corresponding to the increasing ionic strength can be readily achieved. Preliminary testing of this method with mAb molecules showed great promise. Therefore, this salt gradient method was selected for further development and evaluation. It is worth noting that 300 mM ammonium acetate can be well tolerated by this platform, as evidenced by high quality raw mass spectra for both high- and low-abundance species at varying retention times (Figure S3).

Optimization of Column Temperature for the AEX-MS Method. Two mAb molecules (mAb-A with *pI* = 6.6 and mAb-B with *pI* = 6.8) were tested by AEX-MS at column temperatures of 25, 35, and 45 °C, respectively, to study the effect on mAb retention and separation. A previous study on the salt gradient CEX method has indicated that lower column temperatures (i.e., 30 °C) were more favorable for mAb separation compared to higher temperatures (i.e., 60 °C), exhibiting slightly higher peak capacity.[16] Interestingly, for our AEX method, both mAb molecules exhibited significantly improved variant separation, as well as sharper peaks, as the column temperature increased from 25 to 45 °C (Figure 1). In addition, the overall retention of both mAbs increased slightly at elevated column temperatures, which was likely related to the surface charge shifts due to high temperature-induced changes in mAb higher order structure. Although mAb molecules are generally thermally stable with melting temperatures well above 50 °C,[28] it is possible that partial unfolding of some local structures can still occur at mildly elevated temperatures, thereby increasing the solvent accessibility of some acidic residues, as well as their interactions with the AEX resin. Because of the improved chromatographical resolution at 45 °C, the basic and acidic variants of both mAbs can be readily identified and quantified (Table S1). Therefore, the column temperature of 45 °C was selected for the AEX-MS analysis of intact mAbs.

Evaluation of the AEX-MS Method Suitability. To test the method suitability, seven in-house mAbs (IgG1 and IgG4 subclasses) and NISTmAb, with p*I*s ranging from 6.1 to 9.2, were subjected to the native AEX-MS analysis. The generated total ion chromatograms (TICs) are shown in Figure 2, where each separated variant peak was labeled and identified based on accurate mass measurement and empirical knowledge (Table S2). As expected, better variant separation was achieved for mAb molecules with lower p*I*s. The two most basic

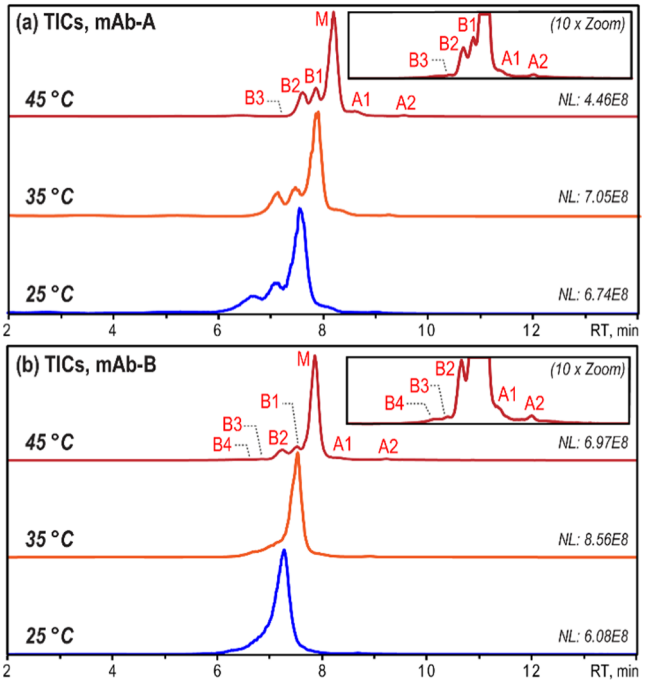

Figure 1. TIC traces from native AEX-MS analysis of (a) mAb-A (p*I* = 6.6) and (b) mAb-B (p*I* = 6.8) at column temperatures of 25 °C (blue trace), 35 °C (orange trace), and 45 °C (red trace). Zoom-in views of the TIC traces at 45 °C are shown in the insets.

molecules, mAb-7 and NISTmAb, which are also IgG1-based mAbs, showed poor retention and resolution. In contrast, good separation was achieved for all six IgG4-based mAbs (mAb-1 to mAb-6) with relatively low p*I*s. Interestingly, even though mAb-6 has a p*I* (p*I* = 7.3) higher than the mobile phase pH, decent separation was still achieved, suggesting it is the surface charge rather than the intrinsic charge that dictates the AEX separation. The acidic variants separated and identified in the AEX-MS analysis include deamidation, glycation, glucuronylation, and sialic acid (Neu5Ac)-containing species (Table S2), which are largely consistent with the commonly observed acidic variants from both the CE-MS and CEX-MS methods.[29,30] Interestingly, deamidated variants were found in multiple acidic peaks for all of the surveyed IgG4 mAbs. For example, mAb-1 exhibited an abundant A1 peak containing deamidation, which correlated well with a known deamidation site in its complementarity-determining regions (CDRs) (~26% deamidation by peptide mapping analysis, data not shown). For mAb-2 through mAb-6, two deamidation peaks (A1 and A2) were observed that showed a highly comparable elution pattern. As these molecules lack deamidation sites in the CDRs, these two peaks (e.g., A1 and A2) are likely attributed to site-specific deamidations in the Fc region. This hypothesis was further studied and supported in the later sections. The basic variants identified in the AEX-MS analysis include unprocessed C-terminal Lys (e.g., C-term K), non-cyclized N-terminal glutamine (e.g., N-term Q), succinimide, and mAb species with varying number of Fc *N*-glycans (Table S2). In addition, specific glycoforms such as Man5/Man5 with an unprocessed C-term K and G0F/G0F-GlcNAc were effectively separated as basic variants in mAb-1. In particular, the developed AEX-MS method is highly sensitive to the Fc *N*-glycosylation macroheterogeneity, where fully, partially, and nonglycosylated mAb species can be well separated. For

https://doi.org/10.1021/acs.analchem.2c00707
Anal. Chem. 2022, 94, 6355−6362

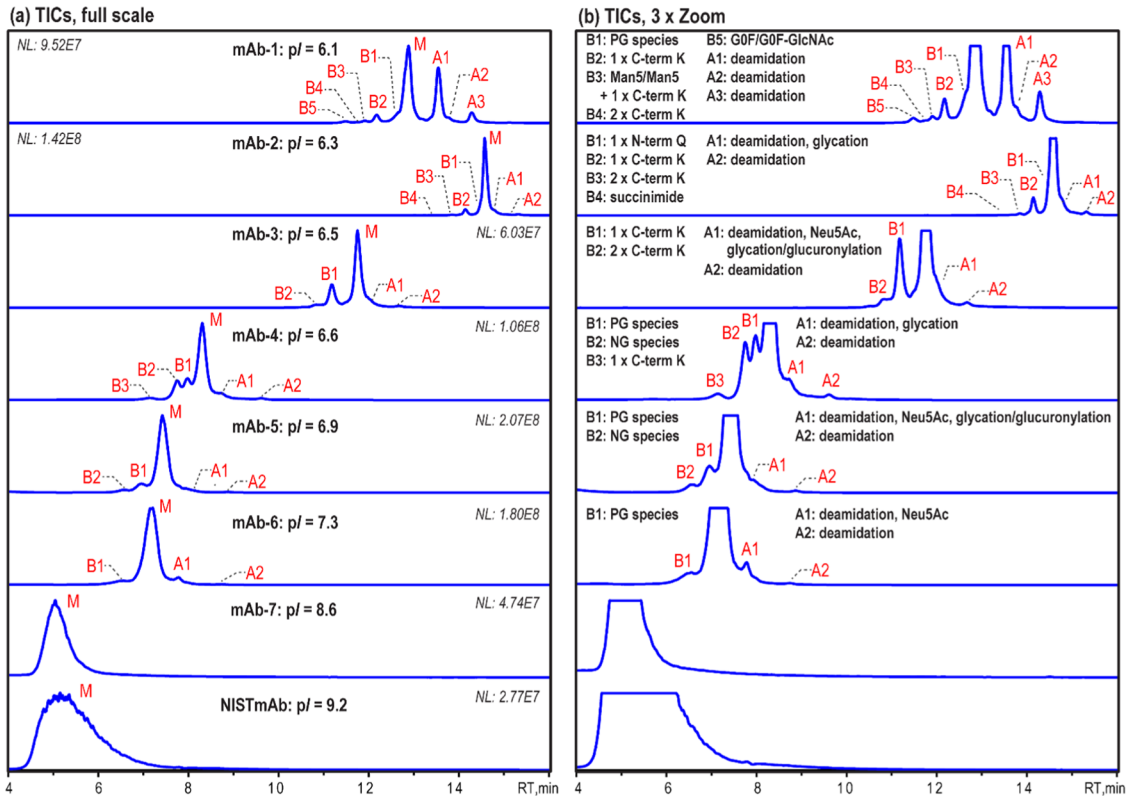

Figure 2. (a) TIC traces from native AEX-MS analysis of different mAb molecules (5 μg injection) with p*I* values ranging from 6.1 to 9.2. (b) A zoom-in view of the TIC traces is displayed on the right. Charge variant peaks are denoted as follows: M, main; A, acidic; and B, basic.

example, in the cases of mAb-4 and mAb-5, the non-glycosylated (NG: none of the two Fc *N*-glycosylation sites are occupied) and the partially glycosylated (PG: one of the two Fc *N*-glycosylation sites is occupied) mAb species eluted in B2 and B1 peaks, respectively, both of which were earlier than the fully glycosylated (FG: two of the two Fc glycosylation sites are occupied) main species. This achieved separation is likely driven by surface charge differences of mAb molecules with different Fc *N*-glycosylation status, which is known to have a large impact on the mAb higher order structure.[31]

Compared to the reported CEX-MS and CE-MS methods, the ability to separate mAb variants based on Fc *N*-glycosylation is advantageous, as it is a critical quality attribute that can impact both the biological function and stability of mAb molecules.[32,33] Overall, although the developed native AEX-MS method is not suitable for IgG1 molecules with high p*I*s, it is broadly applicable to IgG4-based molecules with moderate p*I*s, and offers some unique selectivity compared to other methods.

Comparison of CEX-MS and AEX-MS Methods. The charge heterogeneity of mAbs are highly complex. Therefore, its characterization can benefit tremendously from orthogonal separation techniques with different selectivities. Although the CEX-MS method has been extremely successful in this task, its separation performance reduces considerably for relatively acidic mAbs, which include a significant portion of IgG4-based molecules. To demonstrate the utility of the developed AEX-MS method in these scenarios, an IgG4-based mAb molecule with p*I* = 6.8 was analyzed using both the CEX-MS (Figure 3a) and AEX-MS methods (Figure 3b). From the CEX-MS analysis, two acidic peaks (A1 and A2), which both showed

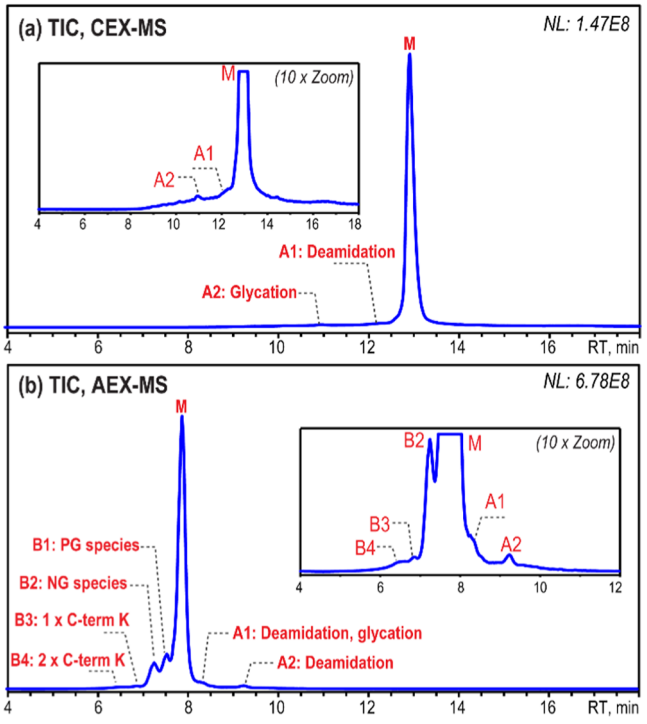

Figure 3. Comparison of (a) CEX-TIC and (b) AEX-TIC of an IgG4 mAb (p*I* = 6.8). Zoom-in views are shown as insets. The column temperature was 45 °C. Charge variant peaks are denoted as follows: M, main; A, acidic; and B, basic.

broad elution, were identified as deamidated and glycated variants, respectively (Table S3a). On the other hand, no

https://doi.org/10.1021/acs.analchem.2c00707
Anal. Chem. 2022, 94, 6355−6362

obvious basic variants were observed, although a low level of unprocessed C-terminal Lys was expected for this molecule (2.5% by peptide mapping analysis, data not shown). In contrast, AEX-MS analysis of the same mAb readily resolved four basic variants, including mAb species with 1 or 2 unprocessed C-terminal Lys, as well as partially and non-glycosylated mAb species. Because of the improved chromatographical resolution, high quality native MS spectra could be obtained for these low-abundance variants with little interference from the main species, leading to highly confident identification. Furthermore, AEX-MS analysis also revealed two acidic peaks, where A1 consisted of both deamidated and glycated variants while A2 was attributed to another deamidation (Table S3b). Similar to other mAb molecules discussed earlier, it is likely that the AEX-MS method provided separation for site-specific deamidation variants. Overall, for this IgG4-based mAb molecule, the AEX-MS method exhibited better variant separation compared to the CEX-MS method, enabling more sensitive and confident charge heterogeneity characterization. Therefore, for mAb molecules that have low p*I*s and are not well separated by CEX, AEX-MS method can be an attractive alternative. Because of its unique selectivity toward Fc *N*-glycosylation and deamidation, AEX-MS method could also be applied in parallel with the CEX-MS method to achieve a more comprehensive charge heterogeneity characterization.

Improving AEX-MS Resolution by PNGase F-Mediated Deglycosylation. During the evaluation of the AEX-MS method suitability, it was found that better AEX separation was achieved for mAb molecules with lower p*I*s. Therefore, we sought to explore the possibility of improving the AEX separation by lowering mAb p*I*s through sample treatment. One straightforward approach is to take advantage of the PNGase F-mediated deglycosylation reaction, which removes *N*-glycans and simultaneously converts the glycan-bearing asparagine (Asn) residue to aspartic acid (Asp) residue. As all IgG4 mAbs contain a conserved Fc *N*-glycosylation site in each of the two heavy chains, this treatment conveniently introduces up to two Asn to Asp conversions, and therefore, effectively lowers the p*I*s. To test this strategy, three mAb molecules (mAb-3 with p*I* = 6.5, mAb-4 with p*I* = 6.6, and mAb-8 with p*I* = 6.9) were subjected to AEX-MS analysis both before and after PNGase F treatment, and the resulting total ion chromatograms (TICs) are presented in Figure 4. Upon PNGase F treatment, it is evident that the overall AEX retention of all three mAb molecules improved significantly, confirming the increased acidity resulting from the Asn to Asp conversions. In addition, notable improvements in both peak sharpness and variant separation were achieved for all three molecules after the treatment. Interestingly, because the fully, partially, and nonglycosylated mAb species carried a descending number of Asn to Asp conversions (e.g., 2 × conversions for fully glycosylated mAb, 1 × conversion for partially glycosylated mAb, and 0 × conversion for non-glycosylated mAb) after PNGase F treatment, they were sequentially separated on AEX column due to the altered acidity. This is the most evident in the case of mAb-4 (Figure 4, middle panel). Upon the treatment, the retention time of the fully glycosylated mAb (M peak) shifted to later by ∼1 min due to increased acidity from 2 × Asn to Asp conversions, while the retention time of the partially glycosylated mAb (B1 peak) only shifted by ∼0.5 min due to increased acidity from 1 × Asn to Asp conversion. In contrast, the retention time of the nonglycosylated mAb (B2 peak) remained unchanged after the PNGase F treatment, as no conversion would have occurred. As a result, even after removing the Fc *N*-glycans, the Fc *N*-glycosylation macroheterogeneity can still be effectively characterized by this AEX-MS method. Because of the improved chromatographical resolution, a couple of minor variants that were previously beyond detection by the AEX-MS method were successfully identified after PNGase F treatment. For example, both B1a peaks in mAb-3 and mAb-8 were identified as partially glycosylated species (with 1 × Asn to Asp conversion), which were separated from other charge variants only after PNGase F treatment. (Table S4). Therefore, PNGase F-mediated deglycosylation was demonstrated as an effective approach to improve the chromatographical performance of the AEX-MS method.

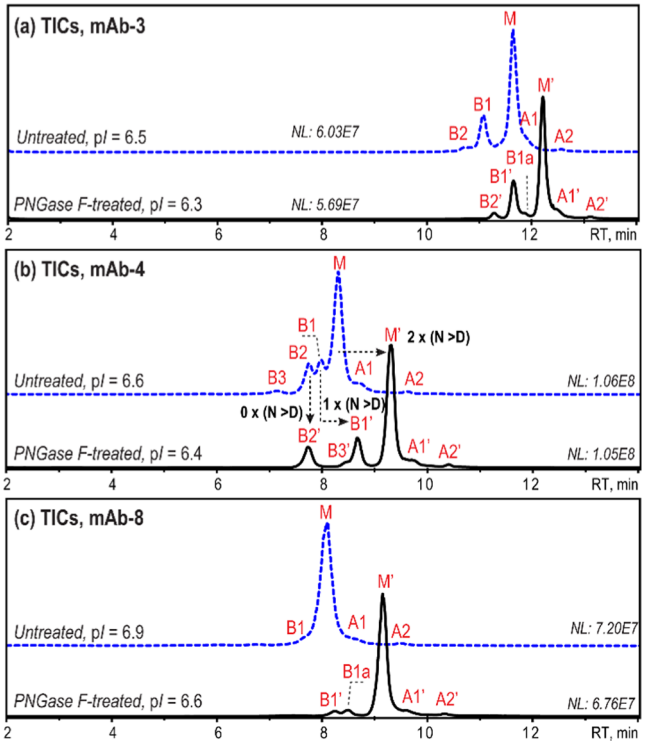

Figure 4. TIC traces from native AEX-MS analysis of (a) mAb-3, (b) mAb-4, and (c) mAb-8 before (dashed blue trace) and after (solid black trace) the PNGase F treatment. Charge variant peaks are denoted as follows: M, main; A, acidic; and B, basic. N, asparagine; D, aspartic acid.

Application of the AEX-MS Method for IgG4 Fc Attribute Monitoring. We next evaluated the application of the AEX-MS method for IgG4-based mAb subunit analysis. After IdeS digestion, it was found the F(ab′)$_2$ fragments from most IgG4 molecules were poorly retained or separated on the AEX column, likely due to their relatively high p*I*s. In contrast, the AEX-MS analysis of the Fc fragments showed excellent chromatographical resolution, with multiple variant species baseline-resolved. Hence, we sought to explore the utility of the AEX-MS method for IgG4 Fc attribute monitoring. To monitor the Fc *N*-glycosylation occupancy, the released Fc fragments were also treated with PNGase F-mediated deglycosylation. Unlike analysis at intact mAb level, initial testing indicated that a column temperature of 25 °C instead of 45 °C was preferred for the analysis of Fc fragments, exhibiting improved peak shape and variant separation (Figure S4). As

https://doi.org/10.1021/acs.analchem.2c00707
Anal. Chem. 2022, 94, 6355−6362

shown in Figure 5a, AEX-MS analysis of the IdeS-released and deglycosylated Fc fragments from mAb-4 revealed four basic

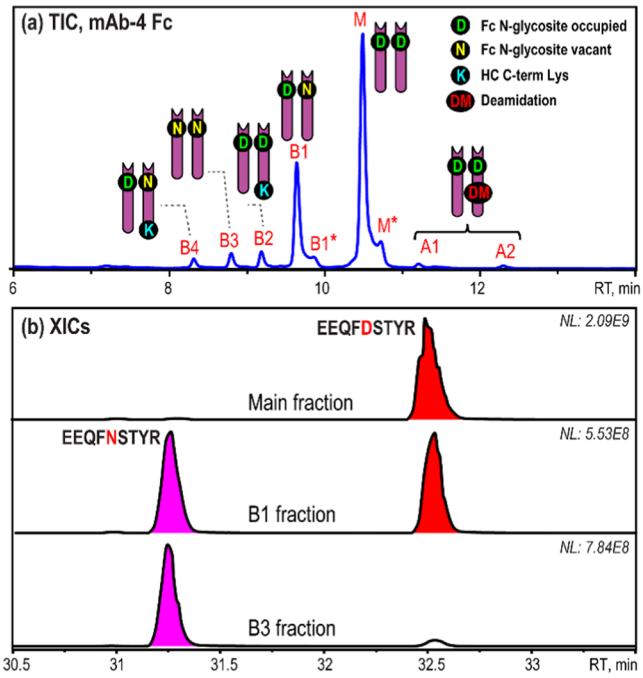

Figure 5. (a) TIC trace from AEX-MS analysis of the IdeS-released and deglycosylated Fc fragments from mAb-4 (IgG4). (b) XICs of the native and deamidated forms of Fc *N*-glycosite containing tryptic peptide (EEQFNSTYR) from peptide mapping analysis of the Main, B1, and B3 fractions. All isotopes and charge states of both peptides were used to generate the XICs. Charge variant peaks are denoted as follows: M, main; A: acidic; and B: basic.

variants (B1, B2, B3, and B4) and two acidic variants (A1 and A2), which were all baseline-resolved. Consistent with the AEX separation of the intact and deglycosylated mAbs, the main, B1, and B3 peaks were attributed to fully glycosylated Fc (with 2 × Asn to Asp conversions), partially glycosylated Fc (with 1 × Asn to Asp conversion), and nonglycosylated Fc (with 0 × Asn to Asp conversion), respectively. The observed mass differences between these species (main: 47543.0 Da; B1: 47542.0; B3: 47541.0 Da) also correlated very well with the number of Asn to Asp conversions, which resulted in a mass increase of ∼0.98 Da per conversion (Table S5). To fully confirm these assignments, the B1, B3, and main peaks were fractionated, digested by trypsin, and subjected to LC-MS/MS analysis. The tryptic peptide containing the Fc *N*-glycosite was then analyzed to determine the relative abundances of the native (EEQF*N*STYR) and deamidated (EEQF*D*STYR) forms. The extracted ion chromatograms (XIC) of both forms are shown in Figure 5b, and the quantitation results are summarized in Table S6. It is clear that the main peak showed almost entirely the deamidated form, confirming its identity as fully glycosylated Fc, with both *N*-glycosites being occupied and converted to Asp. The B1 peak showed approximately 50% deamidated form, confirming its identity as partially glycosylated Fc with one of the two *N*-glycosites being occupied and converted to Asp. Finally, the B3 peak showed almost entirely the native form, confirming its identity as nonglycosylated Fc with none of the two *N*-glycosites being occupied. Subsequently, based on accurate mass measurement, the B2 peak was identified as fully glycosylated Fc with one unprocessed C-term Lys, while B4 peak was identified as partially glycosylated Fc with one unprocessed C-term Lys. Interestingly, a tailing shoulder peak was also observed for both the main peak (M*) and the B1 peak (B1*), each of which showed an identical mass to its preceding peak (Figure 5a, Table S5). Therefore, it is speculated that this shoulder peak was likely attributed to a conformational isomer. As all of these basic variants are baseline-resolved by AEX separation, it is feasible to use this method to directly quantify the levels of unprocessed C-terminal Lys and *N*-glycosylation occupancy at Fc level. To achieve accurate quantitation, the UV peak areas from AEX separation were used for calculation, and the results were compared to that from the peptide mapping analysis (Table S7). Using this approach, the unprocessed C-terminal Lys was determined to be 3.7%. This value is notably lower than that from the peptide mapping analysis (9.8%), which is known to overestimate the C-terminal Lys levels due to significantly higher ionization efficiency of the Lys-containing peptide.[34] Meanwhile, the Fc *N*-glycosylation occupancy was determined to be 29.8% by the AEX method, compared to 25.8% from peptide mapping analysis. These values overall agreed well with each other, considering the two approaches were largely different and used multiple assumptions (e.g., quantitation by peptide mapping assumes equal ionization efficiency for different peptides). Consistent with the AEX-MS analysis of the intact mAbs, two deamidated variants (A1 and A2 peaks) were well separated and identified at Fc level (Figure 5a, Table S5). Complete elucidation of these deamidated variants requires offline fractionation, followed by peptide mapping analysis.

To facilitate the fractionation, a thermally stressed IgG4 mAb-8, which contained significantly elevated levels of deamidation, was subjected to AEX-MS analysis after IdeS digestion and deglycosylation (Figure 6). Again, the basic Fc variants of this molecule were attributed to unprocessed C-terminal Lys and Fc *N*-glycosylation macroheterogeneity, all of which remained unchanged after thermal stress. In contrast, a notable increase in acidic peaks, which were entirely attributed

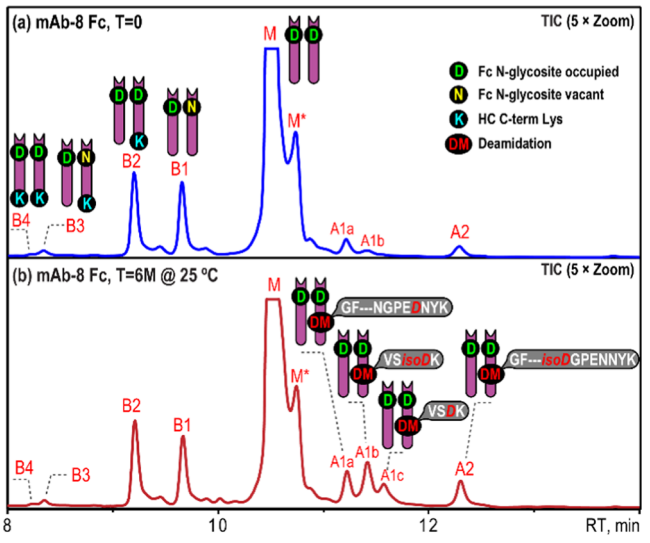

Figure 6. TIC traces from AEX-MS analysis of the PNGase F and IdeS-treated mAb-8 (IgG4) at (a) T = 0 and (b) T = 6 M @ 25 °C. Charge variant peaks are denoted as follows: M, main; A, acidic; and B, basic.

https://doi.org/10.1021/acs.analchem.2c00707
Anal. Chem. 2022, 94, 6355−6362

to deamidation, was observed after the stress (Table S8). Compared to the analysis at intact mAb level, AEX-MS analysis of the Fc fragments exhibited greatly improved resolution in separating these deamidated variants. In total, four deamidation-related acidic peaks (A1a, A1b, A1c, and A2) were resolved from this analysis. As only a few commonly observed deamidation sites are present in IgG4 Fc region (i.e., NG at VVSVLTVLHQDWLNGK;[35] NK at VSNK;[36] NG and NN at GFYPSDIAVEWESNGQPENNYK),[35,37] it is likely that this AEX method is capable of separating site-specific deamidations. To fully elucidate the deamidated variant in each peak, the A1a, A1b, A1c, A2, and the main peaks were fractionated using the thermally stressed sample and subjected to peptide mapping analysis. After tryptic digestion, the deamidated peptides and deamidation sites were readily identified by LC-MS/MS analysis. The differentiation between Asp- and isoaspartic acid (isoAsp)-containing products was achieved by retention time alignment using synthetic peptide standards (Figures S5−S7). The relative abundance of each deamidation was calculated across fractions and then summarized in Table S9. Interestingly, although A1b and A1c fractions were both found to contain deamidation in VS*N*K peptide, A1b fraction mostly contained the isoAsp form, while A1c fraction mostly contained the Asp form. The ability to separate deamidated isoforms at Fc level by AEX method is quite intriguing, considering it is a relatively minor difference (Asp vs isoAsp) within a ∼50 kDa species. We hypothesize that this deamidation site is in direct interaction with the AEX ligand, where Asp form exhibits stronger binding, likely due to a more favorable steric interaction afforded by the longer side chain compared to the isoAsp form. In addition, the dramatic increase of both A1b and A1c peaks in the stressed sample also agreed well with the literature, where VSNK was known to be a deamidation hotspot under thermal stress.[36,38] Subsequently, the A1a fraction was found to show enrichment of Asp-containing product from deamidation of the *N*N site in PENNY peptide. The A2 fraction was found to mostly contain the isoAsp-containing product from deamidation of the *N*G site in PENNY peptide. Separation of these two site-specific Fc deamidation products (A1a and A2) has also been previously demonstrated in a weak anion exchange method using conventional salt buffers.[39] Although the observed elution order was consistent, this developed AEX-MS method exhibited significantly better chromatographical resolution, allowing the separation and detection of additional deamidation products (e.g., VS*D*K and VS*isoD*K). The ability to achieve site-specific and isoform-resolved separation of deamidation products at Fc level is exciting, as it provides a simple means to monitor these attributes without performing peptide mapping analysis, which is time-consuming and known to introduce deamidation artifacts. We then compared the quantitation results from the AEX method with that from the peptide mapping analysis of the unfractionated, stressed sample. As shown in Table S10, although the deamidation levels obtained by peptide mapping analysis were consistently higher, likely due to sample preparation-induced artifact, the two approaches showed highly comparable distributions of different deamidation products. For example, peptide mapping analysis of the PENNY peptide revealed only the Asp-containing product at the *N*N site and primarily the isoAsp-containing product at the *N*G site, which were consistent with the assignments of A1a and A2 peaks in AEX method. Previous studies have also shown that these two products were indeed the major deamidation forms in this peptide when the degradation occurred at intact mAb level.[37,39] Furthermore, peptide mapping analysis also revealed that the isoAsp-containing product was significantly more abundant than the Asp-containing product from the deamidation of VS*N*K peptide. This observation was also consistent with the relative peak intensity of A1b (VS*isoD*K) and A1c (VS*D*K) in the AEX method. Therefore, it is demonstrated that the developed native AEX-MS method is a powerful technique for IgG4 Fc attribute monitoring, enabling facile characterization of the unprocessed C-terminal Lys, *N*-glycosylation occupancy, and site-specific and isoform-resolved deamidations.

CONCLUSIONS

Charge heterogeneity characterization of therapeutic mAbs remains a complex task, which can benefit from novel and orthogonal analytical approaches. In this study, we reported the development and optimization of a native AEX-MS method and evaluated its utility in charge variant analysis of mAbs. We demonstrated that for relatively acidic mAb molecules that were not well separated by CEX, AEX-MS method was a promising alternative. In addition to commonly observed charge variants, this method was particularly sensitive to variants caused by Fc *N*-glycosylation macroheterogeneity and site-specific deamidations. We also found that although the developed AEX-MS method was less useful for IgG1-based mAbs, it is broadly applicable to IgG4-based mAbs, which have gained a lot of momentum and are becoming a rapidly growing class of therapeutics, particularly in the immuno-oncology space. For example, there are currently four FDA-approved IgG4 mAb therapeutics targeting PD-1 for cancer treatment: pembrolizumab (Keytruda), nivolumab (Opdivo), cemiplimab (Libtayo), and dostarlimab (Jemperli), and over six additional IgG4-based PD-1 inhibitors are under development.[40] Therefore, as IgG4-based therapeutics continue to evolve, this developed AEX-MS method will become increasingly valuable as an alternative means to provide comprehensive charge heterogeneity characterization. Finally, we also demonstrated that after PNGase F and IdeS digestion, the AEX-MS method exhibited excellent resolving power for multiple attributes in IgG4 Fc region, including unprocessed C-terminal Lys, *N*-glycosylation macroheterogeneity, and deamidations. Most intriguingly, this method enabled site-specific and isoform-resolved separation for common Fc deamidation variants, thus providing an effective approach to quantify them without performing peptide mapping analysis.

ASSOCIATED CONTENT

Supporting Information

The Supporting Information is available free of charge at https://pubs.acs.org/doi/10.1021/acs.analchem.2c00707.

Extended experimental details for CEX-MS and peptide mapping analyses; figures of the native AEX-MS method setup, pH and conductivity plots for AEX-MS method development, native mass spectra, total and extracted ion chromatograms of native AEX-MS analyses; and tables summarizing charge variants observed in AEX-MS analyses, PTM quantitation from AEX-MS and peptide mapping analyses (PDF)

https://doi.org/10.1021/acs.analchem.2c00707
Anal. Chem. 2022, 94, 6355−6362

AUTHOR INFORMATION

Corresponding Author

Shunhai Wang − *Analytical Chemistry Group, Regeneron Pharmaceuticals Inc., New York 10591-6707, United States;* orcid.org/0000-0003-4055-2187; Email: shunhai.wang@regeneron.com

Authors

Anita P. Liu − *Analytical Chemistry Group, Regeneron Pharmaceuticals Inc., New York 10591-6707, United States*

Yuetian Yan − *Analytical Chemistry Group, Regeneron Pharmaceuticals Inc., New York 10591-6707, United States*

Ning Li − *Analytical Chemistry Group, Regeneron Pharmaceuticals Inc., New York 10591-6707, United States*

Complete contact information is available at: https://pubs.acs.org/10.1021/acs.analchem.2c00707

Notes

A.P.L., Y.Y., S.W., and N.L. are full-time employees and shareholders of Regeneron Pharmaceuticals, Inc.
The authors declare no competing financial interest.

ACKNOWLEDGMENTS

This study was sponsored by Regeneron Pharmaceuticals Inc.

REFERENCES

(1) Wang, X.; An, Z.; Luo, W.; Xia, N.; Zhao, Q. *Protein Cell* **2018**, *9*, 74−85.
(2) Liu, H.; Gaza-Bulseco, G.; Faldu, D.; Chumsae, C.; Sun, J. *J. Pharm. Sci.* **2008**, *97*, 2426−2447.
(3) Xu, Y.; Wang, D.; Mason, B.; Rossomando, T.; Li, N.; Liu, D.; Cheung, J. K.; Xu, W.; Raghava, S.; Katiyar, A.; Nowak, C.; Xiang, T.; Dong, D. D.; Sun, J.; Beck, A.; Liu, H. *MAbs* **2019**, *11*, 239−264.
(4) Ahrer, K.; Jungbauer, A. *J. Chromatogr. B: Anal. Technol. Biomed. Life Sci.* **2006**, *841*, 110−122.
(5) Fekete, S.; Beck, A.; Veuthey, J. L.; Guillarme, D. *J. Pharm. Biomed. Anal.* **2015**, *113*, 43−55.
(6) Wu, S. L.; Teshima, G.; Cacia, J.; Hancock, W. S. *J. Chromatogr.* **1990**, *516*, 115−122.
(7) Griaud, F.; Denefeld, B.; Lang, M.; Hensinger, H.; Haberl, P.; Berg, M. *MAbs* **2017**, *9*, 820−830.
(8) Gahoual, R.; Beck, A.; Leize-Wagner, E.; Francois, Y. N. *J. Chromatogr. B: Anal. Technol. Biomed. Life Sci.* **2016**, *1032*, 61−78.
(9) Yan, Y.; Liu, A. P.; Wang, S.; Daly, T. J.; Li, N. *Anal. Chem.* **2018**, *90*, 13013−13020.
(10) Baek, J.; Schwahn, A. B.; Lin, S.; Pohl, C. A.; De Pra, M.; Tremintin, S. M.; Cook, K. *Anal. Chem.* **2020**, *92*, 13411−13419.
(11) Moritz, B.; Schnaible, V.; Kiessig, S.; Heyne, A.; Wild, M.; Finkler, C.; Christians, S.; Mueller, K.; Zhang, L.; Furuya, K.; Hassel, M.; Hamm, M.; Rustandi, R.; He, Y.; Solano, O. S.; Whitmore, C.; Park, S. A.; Hansen, D.; Santos, M.; Lies, M. *J. Chromatogr. B: Anal. Technol. Biomed. Life Sci.* **2015**, *983-984*, 101−110.
(12) Dai, J.; Lamp, J.; Xia, Q.; Zhang, Y. *Anal. Chem.* **2018**, *90*, 2246−2254.
(13) Dai, J.; Zhang, Y. *Anal. Chem.* **2018**, *90*, 14527−14534.
(14) Fekete, S.; Beck, A.; Fekete, J.; Guillarme, D. *J. Pharm. Biomed. Anal.* **2015**, *102*, 282−289.
(15) Füssl, F.; Cook, K.; Scheffler, K.; Farrell, A.; Mittermayr, S.; Bones, J. *Anal. Chem.* **2018**, *90*, 4669−4676.
(16) Fekete, S.; Beck, A.; Fekete, J.; Guillarme, D. *J. Pharm. Biomed. Anal.* **2015**, *102*, 33−44.
(17) Joshi, V.; Kumar, V.; Rathore, A. S. *J. Chromatogr. A* **2015**, *1406*, 175−185.
(18) Goyon, A.; McDonald, D.; Fekete, S.; Guillarme, D.; Stella, C. *J. Chromatogr. B: Anal. Technol. Biomed. Life Sci.* **2020**, *1160*, No. 122379.
(19) Zhang, L.; Patapoff, T.; Farnan, D.; Zhang, B. *J. Chromatogr. A* **2013**, *1272*, 56−64.
(20) Teshima, G.; Li, M. X.; Danishmand, R.; Obi, C.; To, R.; Huang, C.; Kung, J.; Lahidji, V.; Freeberg, J.; Thorner, L.; Tomic, M. *J. Chromatogr. A* **2011**, *1218*, 2091−2097.
(21) Goyon, A.; Excoffier, M.; Janin-Bussat, M. C.; Bobaly, B.; Fekete, S.; Guillarme, D.; Beck, A. *J. Chromatogr. B: Anal. Technol. Biomed. Life Sci.* **2017**, *1065−1066*, 119−128.
(22) Leblanc, Y.; Bihoreau, N.; Chevreux, G. *J. Chromatogr. B: Anal. Technol. Biomed. Life Sci.* **2018**, *1095*, 87−93.
(23) Füssl, F.; Criscuolo, A.; Cook, K.; Scheffler, K.; Bones, J. *J. Proteome Res.* **2019**, *18*, 3689−3702.
(24) van Schaick, G.; Gstottner, C.; Buttner, A.; Reusch, D.; Wuhrer, M.; Dominguez-Vega, E. *Anal. Chim. Acta* **2021**, *1143*, 166−172.
(25) Yan, Y.; Xing, T.; Wang, S.; Li, N. *J. Am. Soc. Mass Spectrom.* **2020**, *31*, 2171−2179.
(26) Hedges, J. B.; Vahidi, S.; Yue, X.; Konermann, L. *Anal. Chem.* **2013**, *85*, 6469−6476.
(27) Konermann, L. *J. Am. Soc. Mass Spectrom.* **2017**, *28*, 1827−1835.
(28) Kohli, N.; Jain, N.; Geddie, M. L.; Razlog, M.; Xu, L.; Lugovskoy, A. A. *MAbs* **2015**, *7*, 752−758.
(29) Du, Y.; Walsh, A.; Ehrick, R.; Xu, W.; May, K.; Liu, H. *MAbs* **2012**, *4*, 578−585.
(30) Dada, O. O.; Jaya, N.; Valliere-Douglass, J.; Salas-Solano, O. *Electrophoresis* **2015**, *36*, 2695−2702.
(31) Krapp, S.; Mimura, Y.; Jefferis, R.; Huber, R.; Sondermann, P. *J. Mol. Biol.* **2003**, *325*, 979−989.
(32) Zheng, K.; Bantog, C.; Bayer, R. *MAbs* **2011**, *3*, 568−576.
(33) Reusch, D.; Tejada, M. L. *Glycobiology* **2015**, *25*, 1325−1334.
(34) Wang, S.; Liu, A. P.; Li, N. *J. Am. Soc. Mass Spectrom.* **2020**, *31*, 1587−1592.
(35) Chelius, D.; Rehder, D. S.; Bondarenko, P. V. *Anal. Chem.* **2005**, *77*, 6004−6011.
(36) Zhang, Y. T.; Hu, J.; Pace, A. L.; Wong, R.; Wang, Y. J.; Kao, Y. H. *J. Chromatogr. B: Anal. Technol. Biomed. Life Sci.* **2014**, *965*, 65−71.
(37) Sinha, S.; Zhang, L.; Duan, S.; Williams, T. D.; Vlasak, J.; Ionescu, R.; Topp, E. M. *Protein Sci.* **2009**, *18*, 1573−1584.
(38) Yan, Q.; Huang, M.; Lewis, M. J.; Hu, P. *MAbs* **2018**, *10*, 901−912.
(39) Ponniah, G.; Nowak, C.; Neill, A.; Liu, H. *Anal. Biochem.* **2017**, *520*, 49−57.
(40) Kaplon, H.; Reichert, J. M. *MAbs* **2021**, *13*, No. 1860476.